



Photocatalytic degradation of Malachite Green Dye and electrochemical studies using ZnO nanoparticles Fabricated from Sulphatobisthiourea Zn(II) complex.

¹Viswanath R, ²Kirthan B.R, ³Suresh C, ⁴Umesh Reddy K, ⁵Nagendra Anik K

¹Department of Chemistry, MES college of arts, commerce and science, 15th cross Malleshwaram, Bengaluru, Karnataka, India

²Department of Chemistry, Kalpataru Institute of Technology, Tiptur, Karnataka, India

³Department of Physics, Government First Grade College, 18th cross Malleshwaram, Bengaluru, Karnataka, India

⁴Department of Physics, Government First Grade College, Hoskote, Karnataka, India

⁵Department of Environmental Science, Government First Grade College, Davangere, Karnataka, India

ARTICLE DETAILS

Article History:

Received Date: 20-03-2026

Revised Date: 23-03-2026

Accepted Date: 24-03-2026

Published Online: 26-03-2026

Keywords

ZnO NPs, PXRD, SEM, Photoluminescence, CV, malachite green.

Corresponding Author

Email: jayanna007@gmail.com

ABSTRACT

Abstract:

The production of ZnO nanoparticles (NPs) from Sulphatobisthiourea Zn(II) complex by Thermal combustion method in pre-heated muffle furnace at 500 °C for about 3 hours without any impurities. Synthesized ZnO NPs were categorized by different physio-chemical techniques such as; P-XRD analysis, FT-IR Spectroscopy, SEM, UV-Visible spectroscopy and Photoluminescence (PL). The Powder XRD spectrum clearly suggested the crystalline nature and purity of the ZnO NPs. All the diffraction peaks were identical to the monoclinic phase structure. SEM micrographs exhibited that the particles were containing spherical shaped nanostructure. The energy gap of the nanoparticle was found to be 4.33 eV, which was determined from the UV-visible absorption spectrum and also the peak was blue shifted in comparison to the bulk material. The FT-IR spectra were used to investigate the structural nature and chemical composition of ZnO-NPs. Consequently, the metal-oxygen frequency was observed for ZnO-NPs, which was in close agreement with that of literature values. The photocatalytic activity of ZnO nanoparticles were studied against Malachite Green dye under visible light irradiation. The obtained data discloses that ZnO showed good photo degradation compare to Zn (II) complex for Malachite Green dye. ZnO nanoparticles are easy and cost effective in preparation, which acts as effective and potential candidate as photo catalyst in industrial dyes degradation and also has biological applications. Further, the NPs are subjected to Electrochemical and impedance Studies that results show good agreement in the presence of ZnO NPs.

1. Introduction

Nanotechnology can be defined as the science and engineering involved in design fabrication, confirmation and application of materials and devices whose smallest function organization in at least one dimension is on the nanometre [1]. Nano materials shows a unique behaviours and the physio chemical properties that diverge from those at macro molecules [2]. These unique properties of the nano materials results the good applications in the various field [3]. Metal oxides nanoparticles performance a very vital role in different areas of Science and technology. Metal oxide nanoparticles are nanoscale particles composed of metal atoms bound to oxygen atoms. nanoparticles have high surface area and the smaller size will exhibit exclusive physical, chemical, and electronic properties. Some common metal oxide nanoparticles comprise titanium dioxide (TiO₂), zinc oxide (ZnO), iron oxide (Fe₂O₃), and copper oxide (CuO), among others shows good result in the various applications [4]. In technological applications, metal oxides nanoparticles are mainly used for the production of microelectronic circuits, sensing materials, electric devices, fuel cells, coatings for the passivation of surfaces against corrosion, and as catalysts [5]. Zinc oxide (ZnO) nanoparticles are a type of metal oxide nanoparticles composed of zinc and oxygen atoms arranged in a crystalline lattice structure. These nanoparticles have garnered significant attention due to their unique properties and versatile applications across various fields. They possess a large surface area-to-volume ratio, leading to enhanced reactivity and surface-related properties [6]. ZnO nanoparticles can be synthesized in various sizes and shapes, which can influence their properties and applications. These nanoparticles are transparent in the visible region, making them fit mainly for optoelectronic applications [7]. While ZnO nanoparticles offer abundant benefits, there are concerns about their potential toxicity to human health and the environment. Literature survey reveals that ZnO nanoparticles can induce cytotoxicity, oxidative stress, and inflammatory responses in cells, raising concerns about their safe use in consumer products and biomedical applications. Proper risk assessment and mitigation strategies are essential to ensure the safe handling, disposal, and use of ZnO nanoparticles while minimizing potential health and environmental risks [8].

Synthetic organic dyes the colorants that are enormously used in the textile industries cause environmental pollutions likely in the aquatic region owing to their non-biodegradability, toxicity and low photocatalytic activity [9]. Photocatalytic degradation of organic pollutants is a process that utilizes photo catalysts to break down organic compounds into smaller, less harmful molecules through oxidation reactions. This technique has gained significant attention for its potential applications in environmental remediation, water purification, and air pollution control. To decrease the pollution caused by the dyes developed a large area of interest in the field of nanomaterials as a modern-day photo catalyst. Among these photo catalysts especially metal oxide has gained large interest due to their electronic structure, optical and photochemical properties [10]. These properties of the nanomaterials have motivated us to take up work related to metal oxide as photocatalytic agent for environmental remediation.

On considering all the above facts, in this present work describes the structural, optical and pollution measurement of ZnO Nano particles formed by combustion method and nanoparticles were characterized by P-XRD, SEM, UV-visible absorption and FT-IR spectroscopy. The PL measurement, photocatalytic degradation with the malachite green dye and the electrochemical studies.

2. Materials and methods.



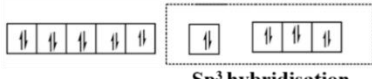
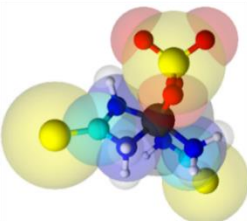
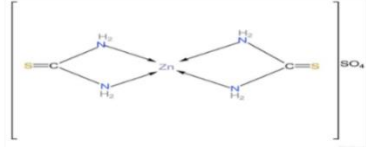
2.1. Chemical and Reagents.

The Zinc sulphate Heptahydrate [ZnSO₄].7H₂O, Con. Sulphuric acid [H₂SO₄], Thiourea [NH₂CSNH₂] and Acetone [CH₃COCH₃] solution and other chemicals and reagents were used to synthesis the metal complex and also for the synthesis of nano materials for further applications were procured from Sigma Aldrich Ltd. Hi-media, Avra chemicals and were used without any purification.

In SHIMADZU model 1650 UV- visible double beam spectrometer in the range of 200– 800 nm in DMF solution recorded the electronic spectra of the compounds. FT-IR spectra (KBr) of the samples were recorded on a Bruker Alpha-T FT-IR Spectrophotometer in the range of 4000– 400 nm. The X-ray powder diffraction patterns were obtained with a SEIFERT model XRD 3000p Powder X-Ray Diffractometer over the range of diffraction angle, 2θ = 5–90 °. The FTIR analysis was recorded by Bruker IFS66V FT-IR spectrometer with a scan range of MIR 100– 4000 cm⁻¹. FE-SEM (ZEISS, EVO 18-2045) was carried out to study nanostructure morphology and size. Optical properties of all the nano powders were performed in the range of 350–500 nm using Shimadzu UV-1800 UV-Vis spectrophotometer. PL spectra were recorded using the PerkinElmer LS55 luminescence spectrometer with a Xenon lamp source. The electrochemical experiments were carried out using CH Instrument-660 with a conventional three-electrode cell. Bare carbon paste electrode (BCPE) and MCPE were used as working electrodes, platinum electrode as a counter electrode, and the saturated calomel electrode (SCE) as the reference electrode.

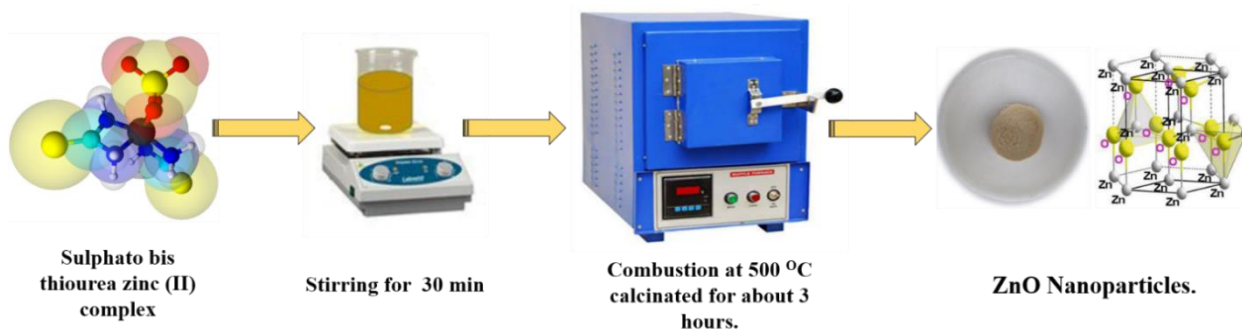
2.2. Synthesis of Sulphatobisthiourea Zn(II) complex.

Sulphatobisthiourea Zn(II) complex was synthesized by taking 3g ZnSO₄, 7 H₂O was dissolved in 10ml of distilled water in the presence of a drop of Con.H₂SO₄ and 3g of Thiourea was dissolved in 20ml of distilled water. To the above Thiourea solution add ZnSO₄ solution drop wise with constant stirring. The obtained crystalline precipitate was filtered using filter paper, then washed it with acetone, the obtained complex was dried in anhydrous CaCl₂.

Flow chart:	Observation
<div style="border: 1px solid black; background-color: #fff9c4; padding: 5px; margin-bottom: 5px;">3g of ZnSO₄.7H₂O dissolved in 10ml distilled water</div> <div style="text-align: center;">↓</div> <div style="border: 1px solid black; background-color: #fff9c4; padding: 5px; margin-bottom: 5px;">Add drop of con. H₂SO₄ + 3g of Thiourea dissolved in 20ml of distilled water</div> <div style="text-align: center;">↓</div> <div style="border: 1px solid black; background-color: #fff9c4; padding: 5px; margin-bottom: 5px;">To Thiourea solution add ZnSO₄ Solution drop wise with constant stirring</div> <div style="text-align: center;">↓</div> <div style="border: 1px solid black; background-color: #fff9c4; padding: 5px; margin-bottom: 5px;">Crystalline ppt is formed</div> <div style="text-align: center;">↓</div> <div style="border: 1px solid black; background-color: #fff9c4; padding: 5px; margin-bottom: 5px;">Dry filter, washed with acetone</div> <div style="text-align: center;">↓</div> <div style="border: 1px solid black; background-color: #fff9c4; padding: 5px;">Dry the ppt and percentage yield is noted</div>	<p>Name of the complex: Sulphato bis thiourea zinc (II) complex [Zn (SCN)] SO₄</p> <p>Electronic configuration of Zn (30): 1s² 2s² 2p⁶ 3s² 3p⁶ 4s² 3d¹⁰</p> <p>Ground state: </p> <p>Excited state: Zn⁺²: 3d¹⁰4s⁰: </p> <p>Hybridisation: </p> <p></p> <p></p>

2.3. Synthesis of ZnO nanoparticles.

ZnO nanoparticles were synthesized by the solution combustion method, here Sulphatobisthiourea Zn(II) complex acts as an oxidizers and lemon juice (citric acid C₆H₈O₇) performed as a fuel. 3.09 g of grinded Sulphatobisthiourea Zn(II) complex was dissolved in a 25 mL lemon juice (25 ml) with constant stirring for about 30 min to attain a homogeneous mixture at ambient temperature, i.e. ~25°C. Then the mixture was dried by keeping it in pre heated muffle furnace at 450°C for about 30 min. Then the obtained product was calcinated at 500°C for 3 h. The calcined sample was allowed to cool in muffle furnace until the sample attained to room temperature and subjected to characterization and application testing. This yield of ZnO nanoparticle which was stored in an airtight container for further analysis.



2.4. Photo-degradation studies.

Photo catalytic degradation studies of ZnO NPs were evaluated under visible light treatment for Malachite Green dye. The testing was implemented with 100 ml of Malachite Green dye solution by means of deionized water. 50 mg of ZnO NPs [Photo catalyst] was added in a 100 ml solution of Malachite Green with an initial concentration of 10 mg/L [11]. The reaction mixture was seethed in the dark condition for about 30 min to achieve the equilibrium. The mixture was exposed at room temperature under a 300 W tungsten visible light lamp. Moreover, the aliquot part was collected at an interval of 15 min to find the degradation percentage of the Malachite Green dye solution [12].

2.5. Electrochemical and impedance studies.

The Cyclic voltammetry and impedance studies of the ZnO nanoparticles was accomplished by means of CHI608E workstation (three-electrode cell) where, ZnO NPs worked as working electrode, the platinum wire was acts as counter and Ag/AgCl as reference electrode [13]. The working electrode was prepared by following the procedure as stated in N. Dhananjaya. Et, al. [14].

3. Results and Discussion.

3.1. Powder X-ray Diffraction (PXRD).

Powder XRD is a quick logical method predominantly used for phase identification of a crystallite material and can provide information on unit cell dimensions. The XRD pattern of the ZnO NPs has been recorded from 10-80° (2θ), revealed in Fig-1. The ZnO NPs crystalline phase was confirmed by typical diffraction peaks at the 2-theta angles of 31.75, 34.51, 36.35, 47.69, 56.68, 62.86, 67.92, and 77.08 according to the standard JCPDS pattern No. 36-1451 [15]. Moreover, the recorded pattern for the as-synthesized ZnO NPs in Fig-1 comprised of this standard pattern and yielded good agreement. Thus, powder XRD peaks were assigned to their corresponding reflection planes of (100), (100), (100), (110), (111), (200), (200), and (210), respectively listed in (Table-1), all peaks were assigned to the corresponding hkl planes. Generally, narrow and sharp XRD peaks appeared for ZnO NPs, showing good sample crystallization, representing that mechanical treatment could not change the crystalline purity of the resulted system. Additionally, Scherer equations was used to estimate the crystallite size of the ZnO NPS sample.

$$D = \frac{k\lambda}{\beta \cos\theta} \quad (1)$$

where λ is the X-ray wavelength radiation (1.5406 Å), β is the full width at half maximum (in radian), and θ is Bragg's angle.

The lattice parameters were analysed by using the following relation,

$$a = d_{hkl} \sqrt{h^2 + k^2 + l^2} \quad (2)$$

Where, d is the interplanar distance between two planes, and h , k , and l are Miller indices.

The d-spacing values were calculated using the X-ray diffraction peaks by the following relation,

$$d_{hkl} = \frac{\lambda}{2 \sin \theta} \tag{3}$$

The dislocation density was determined using the Williamson–Smallman relation,

$$\delta = \frac{1}{D^2} \tag{4}$$

The volume of a unit cell is determined using following relation,

$$V = a^3 \tag{5}$$

The distances between the centers of adjacent ions (the hopping length) in tetrahedral A-sites [L_A] and octahedral B-site [L_B] were determined using the following relations,

$$L_A = \left[\frac{\sqrt{3}}{4} \right] a$$

$$L_B = \left[\frac{\sqrt{2}}{4} \right] a$$

where, a is the lattice parameter

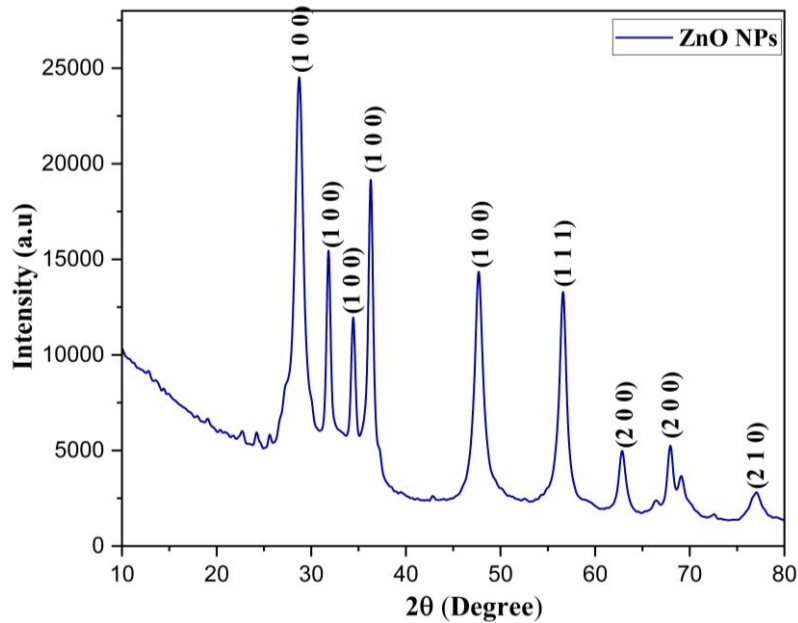


Fig-1: Powder XRD diffraction of ZnO Nanoparticles.

Table-1
The observed 2θ values of XRD data of ZnO Nanoparticles.

2θ	D (nm)	d (Å)	a (Å)	δ (10 ⁻¹⁶)	V (Å ³)	L _A (Å)	L _B (Å)
31.75	6.58	2.81	4.87	2.30	115.90	2.10	1.718
34.51	6.53	2.59	4.87	2.33	115.90	2.10	1.718
36.35	6.50	2.46	4.87	2.36	115.90	2.10	1.718
47.69	6.26	1.90	4.87	2.55	115.90	2.10	1.718
56.58	6.02	1.62	4.87	2.75	115.90	2.10	1.718
62.86	5.84	1.47	4.87	2.93	115.90	2.10	1.718
67.92	5.67	1.37	4.87	3.10	115.90	2.10	1.718
77.08	5.35	1.23	4.87	3.48	115.90	2.10	1.718

3.2. Fourier Transform Infrared (FT-IR) Spectroscopy.

FT-IR spectroscopy is useful in measuring the absorption of FT-IR radiations by a sample, and the results were shown by means of a wavenumber. The evaluation of the IR spectrum includes the correlation of the absorption bands (vibrational bands) and the chemical compounds in the sample [16]. FTIR spectrum analysis gives the information about the functional group of Metal to oxygen bond of as synthesized ZnO nanoparticles in Fig-2.

A number of absorption peaks from 4000 to 400 cm^{-1} corresponds to the carboxylate and hydroxyl impurities in materials and a broad band at 3438.52cm^{-1} was assigned to the O-H stretching vibration mode of hydroxyl group [17]. The peaks observed at 1609 cm^{-1} and 1394 cm^{-1} are due to the asymmetrical and symmetrical stretching of the zinc carboxylate respectively [18]. Meanwhile, the peaks at 1119 cm^{-1} was due to the lattice vibration of carbonate generated absorption peaks

Metal oxides generally exhibit absorption bands in fingerprint region below 1000 cm^{-1} . [19]. The stretching vibration of the Zn–O bond in tetrahedral co-ordination demonstrated an FT-IR absorption peak at about 428 cm^{-1} while it represented a peak at nearly 622cm^{-1} for octahedral arrangement (Table-2). Therefore, FT-IR result has shown to be high purity of synthesized ZnO Nanoparticles. [20]

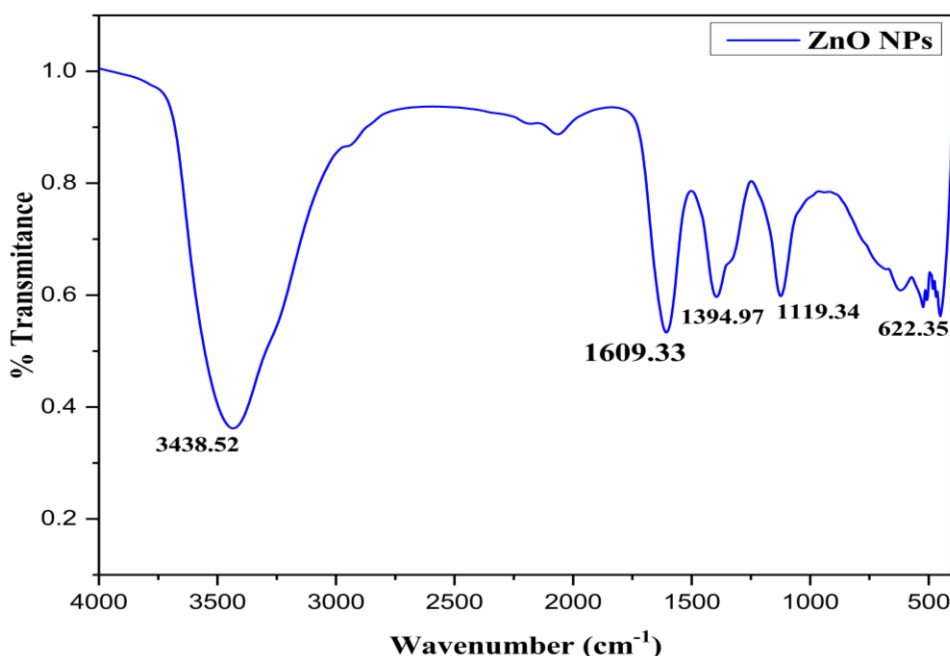


Fig-2: FT-IR spectra for ZnO Nanoparticles.

Table-2
Assignment of FT-IR bands of ZnO Nanoparticles.

Wavenumber (cm ⁻¹)	Stretching frequency
622.35	Zn-O stretching vibration
1119.34	lattice vibration of carbonate generated absorption peaks
1394.97	Symmetrical stretching of the zinc carboxylate
1609.33	Asymmetrical stretching of the zinc carboxylate
3438.52	O-H stretching vibration mode of hydroxyl group

3.3. UV- Visible spectra.

The optical properties of the ZNO NPs studied by using the UV–vis absorption spectra and energy band gap plot for ZnO nanoparticles studied with the help of UV-Visible spectrum which was done in the range of 200-800 nm was showed in the Fig-3 (A). Mainly, the optical properties of the nano particles is examine by using the UV-visible absorption spectroscopy. The UV-Visible spectrum of ZnO Nano particles exhibited an absorption band at about 362.8 nm [21].

An absorption peak is found at about 263.16 nm reveals the ZnO nanoparticles which much lower the band gap wavelength of 362.80 nm ($E_g = 4.33\text{ eV}$) [22]. The absorption peak was recorded in each spectrum in range of 360–

380 nm which is a characteristic band for the pure ZnO. The energy band gap energy is calculated by using the Tauc's plot [23], to get $(\alpha h\nu)^2$ vs $h\nu$ graphs and by extrapolating the linear segment of the curve showed in Fig-3(B). The estimated optical band gap values for pure ZnO is ~ 4.33 eV. It is described that in the UV-Visible Spectrum the intensity of absorption peak is associated with particle size of nanoparticles. As the particle size decreases, absorption peak shifts towards lower wavelength that is blue shift in comparison to bulk.

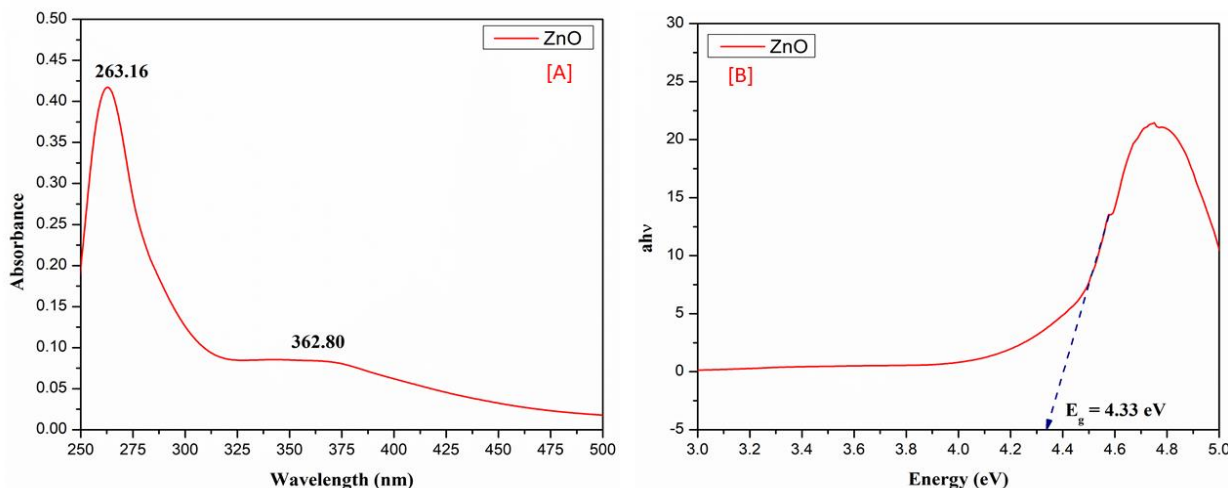


Fig-3. [A] Absorbance in UV-Visible and [B] Energy Band gap spectra for ZnO Nanoparticles.

3.4. Scanning Electron Microscopy (SEM) & EDX.

Scanning Electron Microscopy (SEM) was used to determine the morphology and mean particle size of the synthesized ZnO nano particles. Some SEM images with different magnifications are depicted in Fig-4 (A). The image displays a relatively similar morphology through the sample.

Fig.-4 (A) Displays the SEM images at a higher magnification, and demonstrates the formation of particles with a spongy with a spherical shape. It also provided a clearer idea about the particle. Fig.- 4 (A) illustrate the formation of nanoparticles resulting from the decomposition, as they appear in form of faceted crystals. One of this is its relatively higher porosity. Separation, as the particles are seen to be separated smoothly, without being highly affected by agglomeration. [24-26].

The energy dispersive X-ray (EDX) spectra of ZnO NPS are exposed below, the EDX data gives the elemental composition of the synthesized ZnO NPs. The presence and conformation of each element is given in Tables-3 and Fig-4 (B) and from the EDX spectra from which the corresponding C, O, Zn, Al, and S elements were present in ZnO NPs exposed in Fig-4 (B).

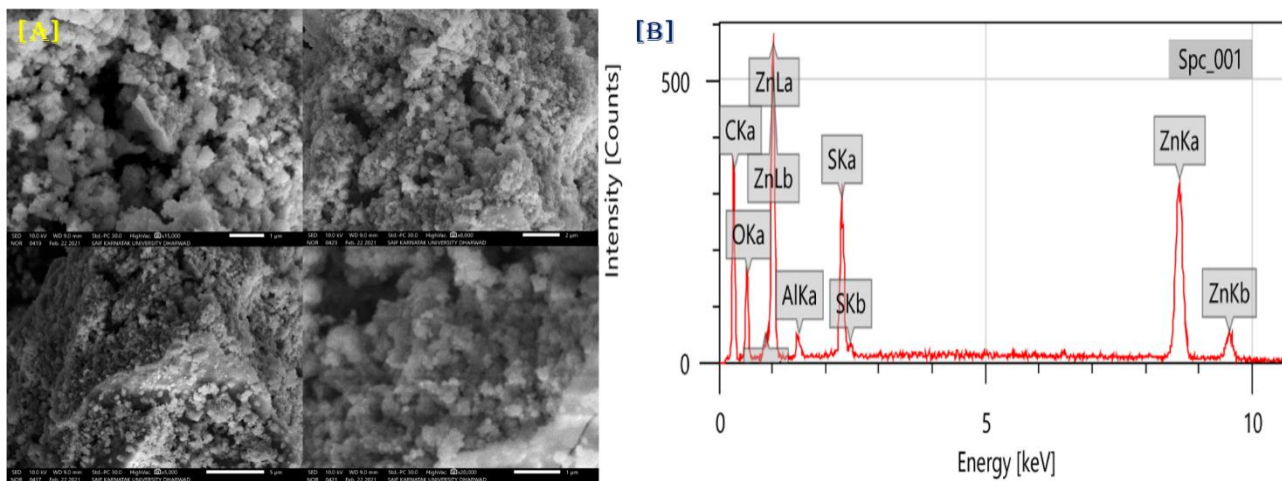


Fig-4. SEM (A) & EDX (B) images of ZnO Nanoparticles for different magnification.

Table-3
Quantified data of ZnO NPs

Element	Line	Mass%	Atom%
C	K	38.17 ± 0.36	67.69 ± 0.64
O	K	10.20 ± 0.27	13.59 ± 0.35
Al	K	0.70 ± 0.06	0.56 ± 0.04
S	K	4.63 ± 0.09	3.08 ± 0.06
Zn	K	46.29 ± 0.70	15.09 ± 0.23
Total		100.00	100.00
Fitting ratio: 0.0514			

3.5. Photoluminescence Study.

Photoluminescence studies comprise the investigation of light discharge from a material after it absorbs light energy. This method is extensively used in several areas, including materials science, physics, chemistry, and biology, to examine the electronic, structural, and optical properties of materials. photoluminescence studies provide valuable insights into the optical properties and behavior of materials, enabling advancements in a wide range of scientific and technological areas [27]. The luminescence spectrum displays two emission peaks, one is found at 347 nm (UV region) corresponding to the near band gap excitonic emission [28] and the other is found at 487 nm recognized to the presence of singly ionized oxygen vacancies [29]. The PL spectra show peaks in blue region around 347 nm and in broad blue region around 487 nm show in (Fig-5). It is known that the PL emission is caused by the recombination of excited electrons and holes, and the lower PL intensity may indicate the lower recombination rate of electrons and holes under light irradiation. The PL intensity is highest as prepared sample, indicating the highest recombination of electrons and holes. It is reasonable that there are some defects in the ZnO nanostructures at the surface and subsurface due to their fast reaction formation process and large surface-to volume ratio. [30]

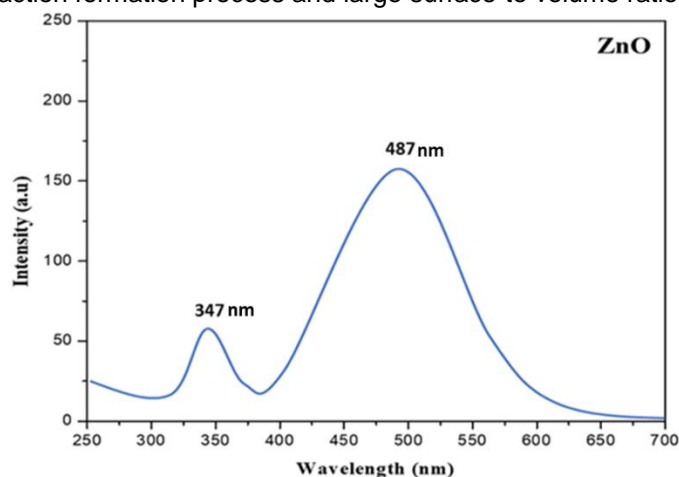


Fig.-5: Photoluminescence study of ZnO Nanoparticles.

3.6. Photo-catalytic study

The photo degradation study of the malachite green dye using ZnO NPs was carried out by using the visible light in a glass reactor having a 400 W mercury vapour lamp. Visible light region was used as the irradiation source in the photo degradation because of the absorption in the visible region enhance the broad peak compared to UV region [31]. The samples were analysed using absorption spectra of the degradation samples of ZnO NPs in the presence of dye (malachite green) at the different time interval of 0 - 120 min showed in Fig -6 [A]. The photocatalytic activity of ZNO NPs is shown that the degradation percentages 94.28 % in the time period of 120 min, which shows evident efficiency of the degradation to Malachite green dye, which regards to charge separation and transport compared to the other ZnO NPs, as exposed in the electrochemical studies.

But, heterogeneous photo catalysis retaining semiconductor oxides and UV-visible light, it converts organic pollutants into moderately harmless end-products as CO₂, H₂O and inorganic ions [32]. Furthermore, photo catalysis agreements

a good auxiliary compare to other conservative methods for water remediation, it uses as a renewable and environmentally favorable source of energy like sunlight.

The photocatalytic activity processes enrich mainly by the physical and chemical properties of nanomaterials. Although, increased in the surface area in conjunction with changes in surface properties nanomaterials role as superior catalysts [33]. Likewise, size imprisonment in creases their optical properties [34]. MG (colour index no. 93405) is an organic dye having chemical formula C₅₂ H₅₄ N₄ O₁₂. MG is a green crystal powder with a metallic luster, extremely soluble in water and ethanol by means of blue green solutions.

The catalytic activity of synthesized ZnO nanoparticles was evaluated by the degradation of MG dye under UV chamber irradiation. The UV–visible absorbance intensity of MG dye in the presence of ZnO nanoparticles at different time intervals and percentage of dye degradation was shown in Fig-6[B]. The obtained result revealed that the synthesized ZnO nanoparticles have able to catalyse MG dye with 85% degradation potential under UV chamber irradiation. The UV–visible absorbance peak intensity around 660 nm decreased with increasing time, indicating the photodegradation of MG. The degradation efficiency as determined using the following relation,

$$\% \text{ Degradation} = 100 \times \frac{A_o - A_t}{A_o}$$

Where A_o and A_t are the absorbance of the dye before and after photocatalytic reaction [35].

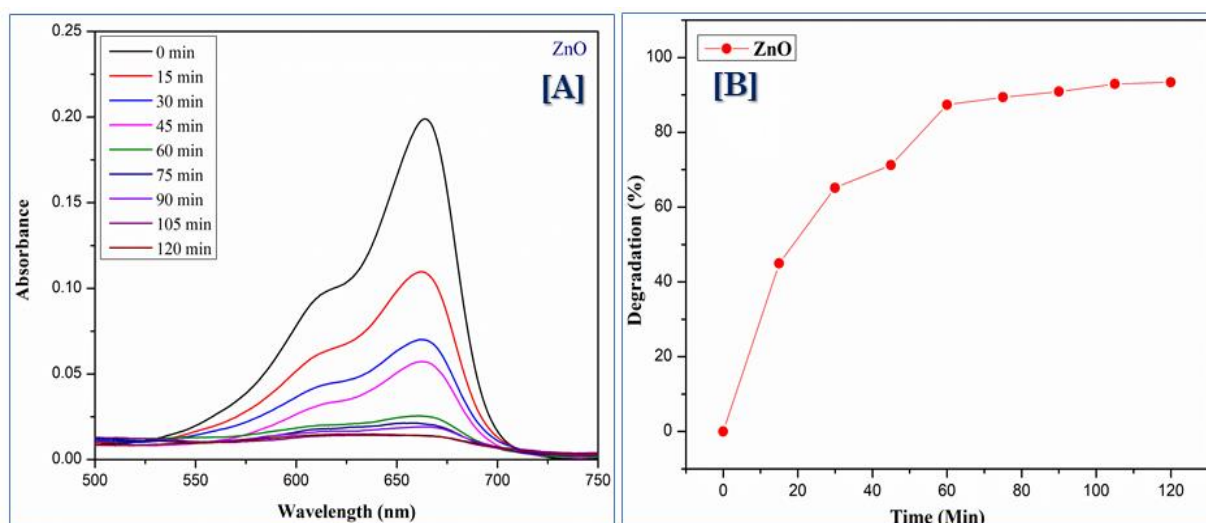


Fig-6: [A] Photocatalytic degradation of Malachite green dye in presences of ZnO & [B] Degradation (vs) time (min) plot of Acid Red dye in presences of ZnO.

3.7. Photodegradation kinetics Study

The photodegradation kinetic studies of ZnO NPs concerning the degradation of malachite green, was assessed by using the Langmuir–Hinshelwood model showed in Fig-7, it designates the rate constant for the photodegradation of malachite green in the existence of ZnO NPs as a photocatalyst and it is resolute by the relation,

$$C_t = C_0 e^{-kt} \text{ (OR) } \ln \frac{C_0}{C_t} = kt$$

where, C₀ is the initial absorbance of malachite green dye solution, C_t is the absorbance of malachite green dye solution at time (t) intervals in the presence of photo catalyst (ZnO NPs), and k is the rate constant.

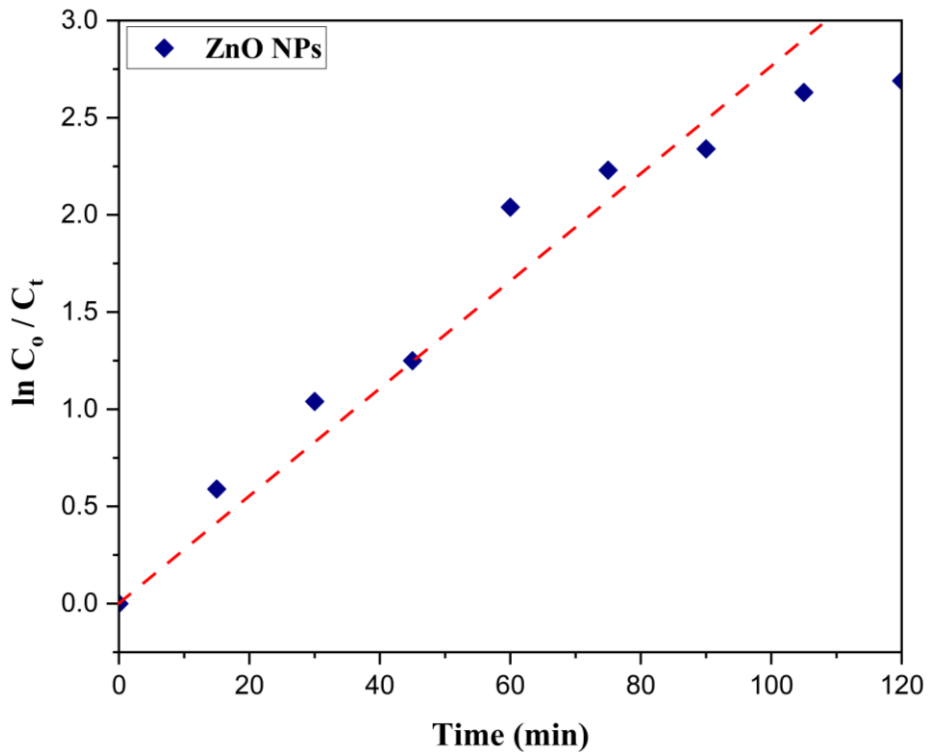
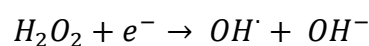
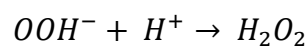
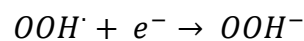
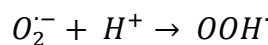
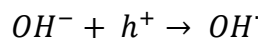
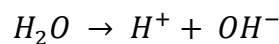
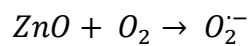
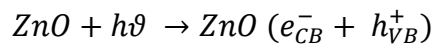


Fig-7: Photo-degradation kinetic studies of ZnO NPs.

3.8. Mechanism action of the Photodegradation.

The mechanism action of photocatalytic degradation of malachite green dye in the existence of ZnO NPs is given in the Fig-8. The visible light falls on the Photocatalyst (ZnO NPs), Due to the photoexcitation, electron (e-) will generating in the conduction band and holes (h+) will generating in the valence band. The holes generated in the valence band will reacts with water surface or hydroxyl ions to form hydroxyl radicals (OH[•]) by photo oxidation, all the same, the electrons generated in the conduction band react with dissolved Oxygen molecules on the surface of the ZnO NPs and forms a superoxide radicals (O₂^{•-}) by photoreduction. An oxidation process in the ZnO NPs will avoid the recombination of e-/h+ pairs in the generated superoxide radicals by maintain the electron neutrality, whereby the superoxide radicals react with e-/h+ pairs, from which H₂O₂ is produced, and then further OH⁻ radicals are recognized. The OH-radicals obtained in the conduction and valence band react with malachite green dye forming CO₂ and H₂O degradation products.

The mechanism action of the photodegradation malachite green dye in the existence of ZnO NPs under the visible light is as given below,



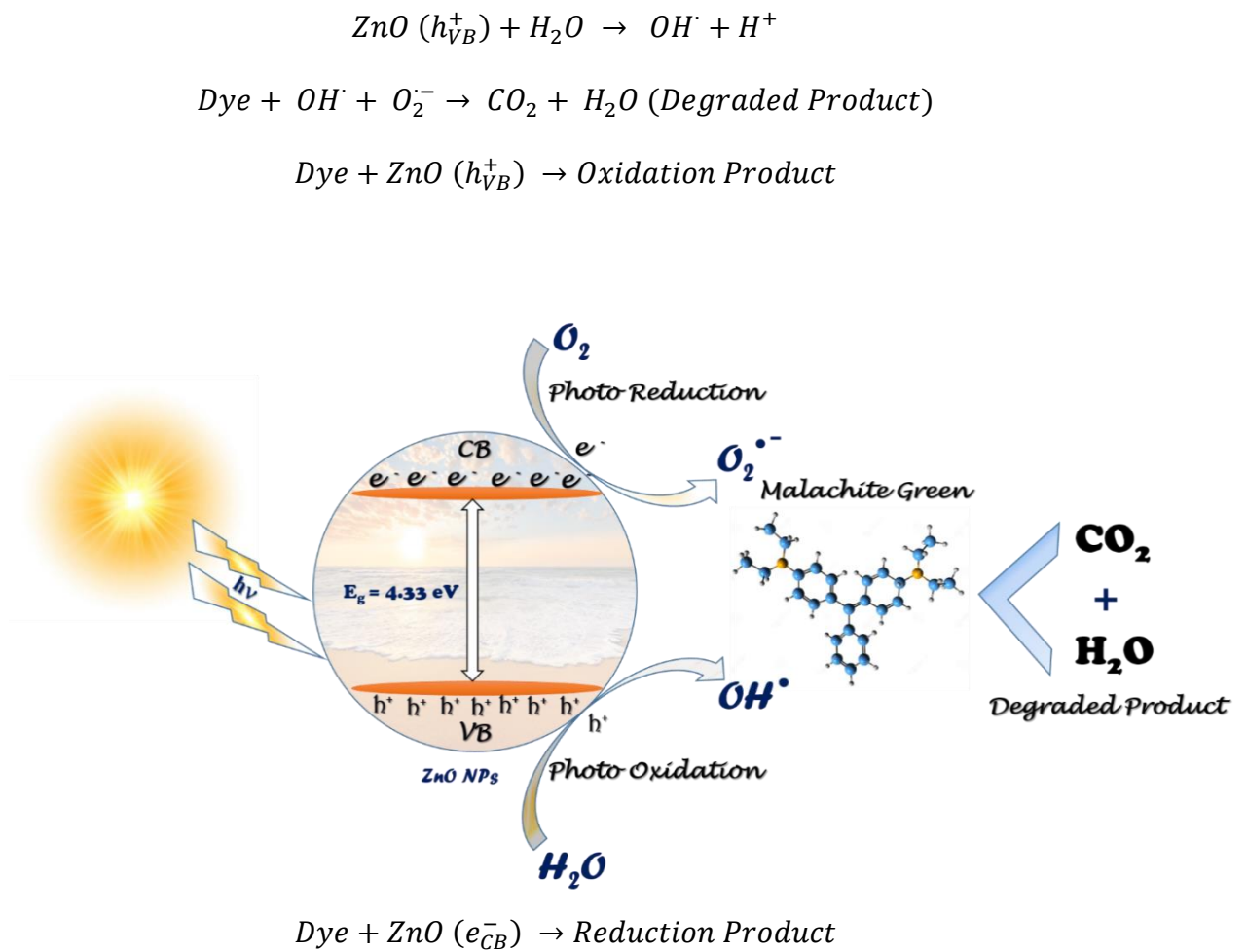


Fig-8: The mechanism action of Photodegradation of malachite green dye in the Presence of ZnO NPs.

3.9. Electrochemical Studies.

The cyclic Voltametric studies of ZnO NPs were conducted at the different scan rates of 0.01, 0.02, 0.04, and 0.05 V/s under the potential range between – 1.0 V to 0.8 V in 0.1 M KOH Aqueouselectrolyte solution [36]. The behavior of the ZnO NPs in the cyclic Voltametricdisplays a reduction peak potential (Epc), associated with the oxidation peaks potential Epa, and separation of this couple (ΔEp) was depicted in Fig-9 [A]. The cyclic voltammety studies indicate

quasi-reversible electron reduction [37], shown in Fig. 9 [A]. The set of strong reveals the redox peaks are raised due to the intercalation/ de-intercalation of alkali metal ion K^+ with the electrode material [38]. The reversible redox reaction of the electrode material is confirmed by the increasing in the anodic and cathodic current with increasing the scan rate [38]. The completion of electrolytic process of an electrode material is decided by the given potential.

Complementary, the AC impedance studies discloses the information about the resistance between the electrode, electrolyte, and the internal resistance [39]. The semicircle region in Fig-9 [B] Exposed that the electron and charge transfer rate of the electrolyte were equal to the electrical resistance. The Nyquist plot of the ZnO NPs electrodes in 0.1 M KOH electrolyte solution done by three-electrode systems. The semicircle district area designates the electron and charge transfer rate in the basic electrolyte. Moreover, the the slope of the curve on behalf of the behavior of a good capacitor which was reliable with the CV results. The above results suggested that the electrolyte can influence the assets like ohmic resistance, electrode resistance, and charge transfer [40].

Overall, the outcome of CV and the impedance studies of ZnO NPs recommended that the electrolyte had a good responsive behaviour regarding electrode resistance, Ohmic resistance and charge transfer. In further investigations, transient photocurrent density measurements were carried out to analyse the charge separation and transport.

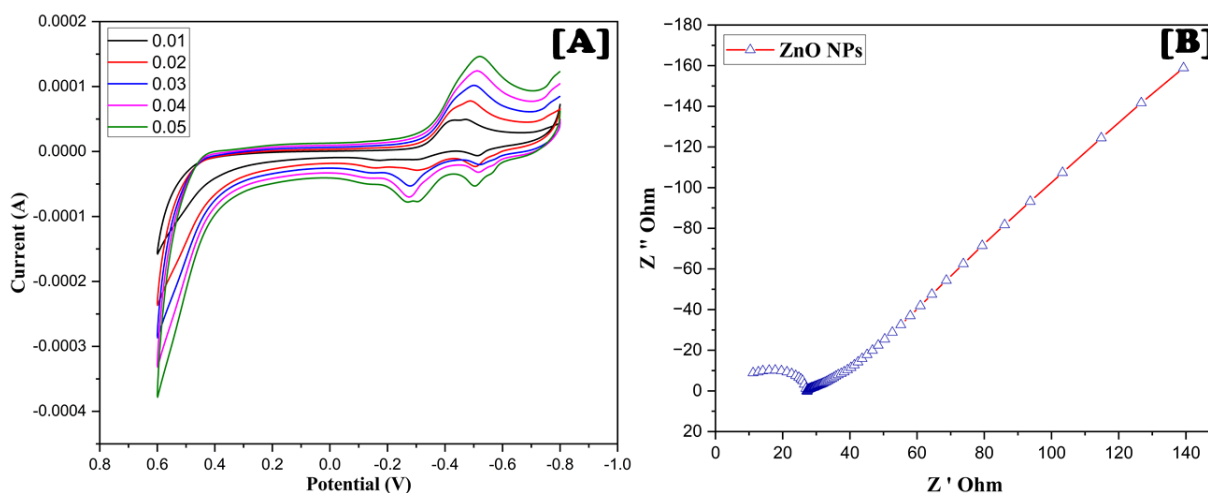


Fig-9: Cyclic Voltammetry [A] & Impedance studies [B] of ZnO NPs.

Conclusion

This studies carried out in this article, concludes ZnO nanoparticles were effectively prepared using Sulphatobisthiourea Zn(II) complex by a combustion method. Powder XRD analysis exposed that the ZnO NPs were scubic in structure with an average crystalline size between 5-7 nm. The synthesized ZnO NPs confirmed the vibrational stretching modes of metal-oxygen bonds using FT-IR spectra. The morphology and elemental composition of the ZnO NPs was found by means of SEM and EDX techniques. UV-Visible analysis confirmed that the ZnO NPs were active materials in visible light and calculated the energy band gap. The Photo Luminescence spectra shown that emission is caused by the recombination of excited electrons and holes. The photo degradation by using the synthesized ZnO NPs showed the good degradation percentage (94.28 %) for a malachite green dye under visible light irradiation. The CV and Impedance studies suggested that the synthesized ZnO NPs was substantial electro-chemical performance regarding electrode resistance, Ohmic resistance and charge transfer. Finally, it concludes that, the ZnO NPs are effective for photocatalytic, optical and also good electronic claims.

References

1. Y. Shao, H.P. Zhao, X.Q. Feng, Optimal characteristic Nano sizes of mineral bridges in mollusk nacre, RSC Adv. 4 (61) (2014) 32451-32456.
2. G. De Crozals, R. Bonnet, C. Farre, C. Chaix, Nanoparticles with multiple properties for biomedical applications: a strategic guide, Nano Today 11 (2016) 435-463.
3. M. Shah, D. Fawcett, S. Sharma, S. K. Tripathy, and G. E. J. Poinern, "Green synthesis of metallic nanoparticles via biological entities," Materials, vol. 8, no. 11, pp. 7278-7308, 2015.
4. Sivaraj, R.; Pattanathu, K.; Rajiv, P.; Hasna, S.; Venckatesh, R. Spectrochim. Biogenic copper oxide nanoparticles synthesis using Leyland NS, Podporska-Carroll J, Browne J, et al. Highly efficient F, Cu doped

- TiO₂ anti-bacterial visible light active photocatalytic coatings to combat hospital-acquired infections. *Sci Rep.* 2016; 6:24770.
5. Pakdel E, Daoud WA, and Sun L, et al. Reprint of: photostability of wool fabrics coated with pure and modified TiO₂ colloids. *J Colloid Interface Sci.* 2015; 447:191–201.
 6. Weir A, Westerhoff P, Fabricius L, et al. Titanium dioxide nanoparticles in food and personal care products. *Environ Sci Technol.* 2013; 46:2242–2250.
 7. Shi D, Sadat ME, Dunn AW, et al. Photo-fluorescent and magnetic properties of iron oxide nanoparticles for biomedical applications. *Nanoscale.* 2015; 7:8209–8232.
 8. Xiong HM. ZnO nanoparticles applied to bioimaging and drug delivery. *Adv Mater.* 2013; 25:5329–5335.
 9. Hou X, Choy KL. Synthesis of Cr₂O₃-based nanocomposite coatings with incorporation of inorganic fullerene-like nanoparticles. *Thin Solid Films* 2008;516(23):8620-4.
 10. M. Ramzan Parra, Z. Fozia Haque, Aqueous chemical route synthesis and the effect of calcination temperature on the structural and optical properties of zno nanoparticles, *J. Mater. Res. Technol.* 3 (4) (2014) 363–369.
 11. K. Elumalai, S. Velmurugan, S. Ravi, V. Kathiravan, S. Ashokkumar, Biofabrication of zinc oxide nanoparticles using leaf extract of curry leaf (*Murrayakoenigii*) and its antimicrobial activities, *Mater. Sci. Semiconduct. Process.* 34 (2015) 365–372.
 12. Rouhi, J.; Mahmud, S.; Naderi, N.; Ooi, C.R.; Mahmood, M.R. Physical properties of fish gelatin-based bio-nanocomposite films incorporated with ZnO nanorods. *Nanoscale Res. Let.* 2013, 8, 364–371.
 13. Padmavathy N, Vijayaraghavan R. Enhanced bioactivity of ZnO nanoparticles– an antimicrobial study. *Sci Technol Adv Mat.* 2008; 9:035004.
 14. N. Dhananjaya, N.P. Ambujakshi, H.R. Raveesha, S. Pratibha, C.R. Ravikumar, Electrochemical Sensor and luminescence applications of *Chonemorpha fragrans* leaf extract mediated ZnO/Ag nanostructures, *Applied Surface Science Advances* 4, 2021, 100075.
 15. N. Talebian, M.R. Nilforoushan, E. Badri Zargar, Enhanced antibacterial performance of hybrid semiconductor nanomaterials: ZnO/SnO₂ nanocomposite thin films, *Appl. Surf. Sci.* 258 (2011) 547–555.
 16. G Vishnu, HS Bhojya Naik, R Viswanath, BR Kirthan, PH Amith Nayak, Mohammed Abdullah Bajiri, Combustion-assisted green-synthesized magnesium-doped cadmium ferrite nanoparticles for multifunctional applications, *New Journal of Chemistry.*,46, 2022, 1943-1959.
 17. E Indrajith Naik, H S Bhojya Naik, R Viswanath, B R Kirthan, M C Prabhakara., Effect of zirconium doping on the structural, optical, electrochemical and antibacterial properties of ZnO nanoparticles prepared by sol-gel method, *Chemical Data collections.*, Chemical Data Collections 29, 2020, 100505.
 18. BR Kirthan, MC Prabhakara, HS Bhojya Naik, PH Amith Nayak, E Indrajith Naik, Synthesis, characterization, DNA interaction and anti-bacterial studies of Cu (ii), Co (ii) and Ni (ii) metal complexes containing azo-dye ligand., *Chemical Data Collections* 29, 2020, 100506.
 19. Barikara Shivaraj, MC Prabhakara, HS Bhojya Naik, E Indrajith Naik, R Viswanath, M Shashank, BE Kumara Swamy, Optical, bio-sensing, and antibacterial studies on Ni-doped ZnO nanorods, fabricated by chemical co-precipitation method, *Inorganic Chemistry Communications* 134, 2021, 109049.
 20. E Indrajith Naik, HS Bhojya Naik, BE Kumara Swamy, R Viswanath, IK Suresh Gowda, MC Prabhakara, K Chetankumar, Influence of Cu doping on ZnO nanoparticles for improved structural, optical, electrochemical properties and their applications in efficient detection of latent fingerprints, *Chemical Data Collections* 33, 2021, 100671.
 21. E Indrajith Naik, HS Bhojya Naik, R Viswanath, IK Suresh Gowda, MC Prabhakara, Bright red luminescence emission of macroporous honeycomb-like Eu³⁺ ion-doped ZnO nanoparticles developed by gel-combustion technique, *SN Applied Sciences* 2, 1-13.
 22. P H Amith Nayak, H S Bhojya Naik, H B Teja, B R Kirthan, R Viswanath, Synthesis, characterization and luminescent properties of mixed-ligand nickel complexes for opto-electronic application, *Journal of Electronic Materials* 50, 2021, 2090-2100.
 23. Kirthan B R, Prabhakara M C, Bhojyanaik H S, Ereshanaik, Viswanath R, Amith Nayak P H, Ravikumar S, Kotresh K R, Fabrication, depiction, DNA interaction, anti-bacterial, DFT and molecular docking studies of Co(II) and Cu(II) complexes of 3-methyl-1-phenyl-4-[(E)-(pyridin-2-yl)diazenyl]-1H-pyrazol-5-ol ligand, *Nucleosides, Nucleotides & Nucleic Acids* 41 (1), 2021, 1-22.
 24. G Arun Kumar, H S Bhojya Naik, R Viswanath, I K Suresh Gowda, K N Santhosh, Tunable emission property of biotin capped Gd: ZnS nanoparticles and their antibacterial activity, *Materials Science in Semiconductor Processing* 58, 2017, 22-29.

25. R Viswanath, HS Bhojya Naik, G Arun Kumar, IK Suresh Gowda, S Yallappa, Tuneable luminescence properties of EDTA - assisted ZnS: Mn nanocrystals from a yellow - orange to a red emission band, *Luminescence* 32 (7), 2017, 1212-1220.
26. Shah Faisal, Hasnain Jan, Sajjad Ali Shah, Sumaira Shah, Adnan Khan, Muhammad Taj Akbar, Muhammad Rizwan, Faheem Jan, Wajidullah, Noreen Akhtar, Aishma Khattak, and Suliman Syed Green Synthesis of Zinc Oxide (ZnO) Nanoparticles Using Aqueous Fruit Extracts of *Myristica fragrans*: Their Characterizations and Biological and Environmental Applications, *ACS Omega*, 6, 2021, 9709–9722.
27. Xian-Qing Zhou, Zakir Hayat, Dong-Dong Zhang, Meng-Yao Li, Si Hu, Qiong Wu, Yu-Fei Cao, Ying Yuan, Zinc Oxide Nanoparticles: Synthesis, Characterization, Modification, and Applications in Food and Agriculture, *Processes*, 11, 2023,1193.
28. S. Hareeshanaik, M. C. Prabhakara, H. S. Bhojya Naik, R. Viswanath, Barikara Shivaraj, G. Vishnu, N. Adarsh gowda,Optical, photo catalytic, electrochemical and antibacterial performance of ZnO and Co doped ZnO nanoparticles, *Inorganic Chemistry Communications*, 158, 2023, 111552.
29. Jitender Josun, Praveen Sharma, Vinod Kumar Garg, Optical and structural behavior of hydrothermally synthesized ZnO nanoparticles at various temperatures with NaOH molar ratios, *Results in Optics*, 14, 2024, 100601.
30. P H Amith Nayak, H S Bhojya Naik, R Viswanath, B R Kirthan, Green light emitting fluorescent [Zn (II)(Schiff base)] complexes as electroluminescent material in organic light emitting diodes, *Journal of Physics and Chemistry of Solids* 159, 2021, 110288.
31. R Viswanath, H S Bhojya Naik, G S Yashavanth Kumar, P N Prashanth Kumar, K N Harish, M C Prabhakara, R Praveen, Synthesis and photoluminescence enhancement of PVA capped Mn²⁺ doped ZnS nanoparticles and observation of tunable dual emission: a new approach, *Applied surface science* 301, 2014, 126-133.
32. B R Kirthan, M C Prabhakara, R Viswanath, P H Amith Nayak, Optoelectronic, photocatalytic and biological studies of mixed ligand Cd (II) complex and its fabricated CdO nanoparticles, *Journal of Molecular Structure* 1244, 2021, 130917.
33. B R Kirthan, M C Prabhakara, H S Bhojyanaik, P H Amith Nayak, R Viswanath, H B Teja, Optoelectronic, Photocatalytic, and DNA interaction studies of synthesised Cu (II), Co (II), and Ni (II) complexes containing schiff base ligand, *Inorganic Chemistry Communications* 135, 2022, 109109.
34. M Madhukara Naik, H S Bhojya Naik, G Nagaraju, M Vinuth, H Raja Naika, K Vinu, Green synthesis of zinc ferrite nanoparticles in *Limonia acidissima* juice: characterization and their application as photocatalytic and antibacterial activities, *Microchemical Journal* 146, 2019, 1227-1235.
35. M Shashank, H S Bhojya Naik, G Nagaraju, Rangappa S K, M Madhukara Naik, K Lingaraju, Facile Synthesis of Fe₃O₄/ZnO Nanocomposite: Applications to Photocatalytic and Antibacterial Activities, *Journal of Electronic Materials* 50, 2021, 3557-3568.
36. M. R. Anil Kumar, Buzuayehu Abebe, H. P . Nagaswarupa, H. C . Ananda Murthy,C. R. Ravikumar, Fedlu Kedir Sabir, Enhanced photocatalytic and electrochemical performance of TiO₂-Fe₂O₃ nanocomposite: Its applications in dye decolorization and as supercapacitors, *Scientific Reports*, 10, 2020, 1249.
37. M.A. Shilpa Amulya, H.P. Nagaswarupa, M.R. Anil Kumar, C.R. Ravikumar, S.C. Prashantha, K.B. Kusuma, Sonochemical synthesis of NiFe₂O₄ nanoparticles: Characterization and their photocatalytic and electrochemical applications, *Applied Surface Science Advances*, 1, 2020, 100023.
38. M.R. Anil Kumar, C.R. Ravikumar, H.P. Nagaswarupa, B. Purshotam, BedasaAbdisa Gonfa, H.C. Ananda Murthy, Fedlu Kedir Sabir, Samson Tadesse, Evaluation of bi-functional applications of ZnO nanoparticles prepared by green and chemical methods, *Journal of Environmental Chemical Engineering*, 2019, 103468.
39. BN Rashmi, Sujatha F Harlapur, B Avinash, CR Ravikumar, HP Nagaswarupa, MR Anil Kumar, K Gurushantha, MS Santosh, Facile green synthesis of silver oxide nanoparticles and their electrochemical, photocatalytic and biological studies, *Inorganic Chemistry Communications* 111, 2020, 107580.
40. M R Anil Kumar, H P Nagaswarupa, C R Ravikumar, S C Prashantha, H Nagabhushana, Aarti S Bhatt, Green engineered nano MgO and ZnO doped with Sm³⁺: Synthesis and a comparison study on their characterization, PC activity and electrochemical properties, *Journal of Physics and Chemistry of Solids* 127, 2019, **127-139**